

A thermodynamic interpretation of the compatibility of chlorinated polyethylene with poly(methylmethacrylate)

Chai Zhikuan and Sun Ruona

Institute of Chemistry, Academia Sinica, Beijing, China

and D. J. Walsh and J. S. Higgins

Department of Chemical Engineering and Chemical Technology, Imperial College of Science and Technology, London SW7, UK

(Received 1 June 1982)

The compatibility of chlorinated polyethylene with poly(methylmethacrylate) and the oligomer analogue chlorinated octadecane with oligomeric PMMA are interpreted using the equation of state theory. It is found that the interaction energy parameter X_{12} and the interaction entropy parameter Q_{12} , obtained from the heat of mixing and the phase boundary of oligomeric mixtures, can be used to generate the phase boundary of the polymer mixture. The spinodals of different molecular weights so generated have less molecular weight dependence than might be expected, in agreement with experimental results. A negative Q_{12} indicates that some ordering may exist in the mixture due to specific interactions.

Keywords Compatibility; polymer blends; interaction parameters; poly(methylmethacrylate); chlorinated polyethylene; phase boundaries

INTRODUCTION

Many papers have been published on the thermodynamics of polymer mixtures. Flory and his colleagues^{1,2} first described the usefulness of the equation of state theory in the analysis of liquid-liquid phase equilibria and the calculation of the thermodynamic functions of polymer mixtures. McMaster³ showed in 1973 that the lower critical solution temperature (*LCST*) can be understood as a common phenomenon in high molecular weight polymer blends. As in polymer solutions, the coexistence of an *LCST* and a *UCST* (upper critical solution temperature) is not impossible. Also, the dependence of the phase diagram on factors such as molecular weights, thermal expansion coefficients, thermal pressure coefficients, the interaction energy parameter and pressure was discussed. In 1978 Patterson and Robard introduced a simple form of the Prigogine-Flory solution thermodynamics⁴. In this, the unfavourable free volume contribution for a compatible high molecular weight system is balanced at low temperatures by a small favourable interactional or contact energy term ($X_{12} < 0$) due to hydrogen bonding or charge transfer. Phase separation is brought about by a decrease of the interaction with increasing temperature. The role of free volume as the cause of the *LCST* is given less emphasis than in the work of McMaster. Some authors have also attempted to simulate the phase boundary of polymer mixtures using the equation of state theory^{5,6}.

The experimental study of phase equilibrium in polymer mixtures is more difficult than in polymer

solutions or solutions of low molecular weight compounds. Extremely slow diffusional processes limit the attainment of equilibrium in the phase separation process. Traditional methods of measuring phase boundaries, free energies of mixing and heats of mixing, etc., are not applicable to polymer mixtures. One way to overcome this difficulty is by studying oligomer pairs⁷. These compounds have similar thermodynamic properties to polymers but their mobility makes it possible to measure phase diagrams, phase volumes, heats of mixing, etc., accurately and directly. Owing to the large combinatorial entropy of low molecular weight compounds, an *LCST* may not be found in these systems. We believe that this will not influence their usefulness as a model to simulate the behaviour of polymer mixtures. Both the *UCST* and *LCST* are a result of a combination of three contributions: combinatorial entropy, equation of state terms and the interaction parameter. Information about these contributions obtained from oligomer systems should be useful for the study of chemically similar systems of high molecular weight.

In a previous communication⁸, we reported some results on mixtures of chlorinated polyethylene (CPE)/poly(methylmethacrylate) (PMMA) and its oligomeric analogue, chlorinated octadecane (COD)/oligomeric methyl methacrylate (OMMA). It was found that CPE with 49.8 and 51.6% chlorine are both compatible with PMMA if the samples are cast from MEK at room temperature and that they exhibit an *LCST*. At lower degrees of chlorination the polymers are not compatible. The compatibility can be explained by the

heat of mixing measured using oligomer pairs which becomes favourable for higher chlorine contents. In this paper the systems will be examined in terms of the equation of state theory. Our purpose is to find the connection between polymer mixtures and their low molecular weight analogues and to explore the characteristics which appear when the theory is applied to the systems. In order to do so, the spinodal is rewritten in a convenient form for calculation. The theory without omitting the pressure term is also presented.

THEORETICAL

In the authors' notation⁹, the Flory equation of state theory gives the free energy of mixing, the heat of mixing and the chemical potential of component 1 as follows:

$$\Delta G_m = \Delta H_m - T\Delta S_m \tag{1}$$

$$\Delta H_m = \bar{r}Nv^*[\phi_1 P_1^*(\tilde{v}_1^{-1} - \tilde{v}^{-1}) + \phi_2 P_2^*(\tilde{v}_2^{-1} - \tilde{v}^{-1}) + \phi_1 \theta_2 X_{12}/\tilde{v}] \tag{2}$$

$$-T\Delta S_m = RT(n_1 \ln \sigma_1 + n_2 \ln \phi_2) + 3\bar{r}Nv^* \{ \phi_1 P_1^* \tilde{T}_1 \ln[(\tilde{v}_1^{1/3} - 1)/(\tilde{v}^{1/3} - 1)] + \phi_2 P_2^* \tilde{T}_2 \ln[(\tilde{v}_2^{1/3} - 1)/(\tilde{v}^{1/3} - 1)] - \bar{r}Nv^* \phi_1 \theta_2 T Q_{12} \} \tag{3}$$

$$\Delta\mu_1 = RT[\ln \phi_1 + (1 - r_1/r_2)\phi_2] + P_1^* V_1^* \{ 3\tilde{T}_1 \ln[(\tilde{v}_1^{1/3} - 1)/(\tilde{v}^{1/3} - 1)] + (\tilde{v}_1^{-1} - \tilde{v}^{-1}) + \tilde{P}_1(\tilde{v} - \tilde{v}_1) \} + (\chi_{12} - TQ_{12}\tilde{v})V_1^* \theta_2^2/\tilde{v} \tag{4}$$

with

$$P^* = \phi_1 P_1^* + \phi_2 P_2^* - \phi_1 \theta_2 X_{12} \tag{5}$$

$$1/T^* = (\phi_1 P_1^*/T_1^* + \phi_2 P_2^*/T_2^*)/P^* \tag{6}$$

and the segment fraction ϕ and interaction site fraction θ are given by

$$\phi_2 = 1 - \phi_1 = r_2 N_2 / \bar{r}N \tag{7}$$

$$\theta_2 = 1 - \theta_1 = S_2 \phi_2 / (S_1 \phi_1 + S_2 \phi_2) \tag{8}$$

Equation (4) is the starting point for deriving the phase boundary of polymer mixtures. The spinodal is given by

$$\partial(\Delta\mu_1/RT)/\partial\phi_2|_{T,P} = 0 \tag{9}$$

i.e.

$$-1/\phi_1 + (1 - r_1/r_2) - (P_1^* V_1^*/RT_1^*)(\partial\tilde{v}/\partial\phi_2)/[\tilde{v}^{2/3}(\tilde{v}^{1/3} - 1)] + (P_1^* V_1^*/RT)(1/\tilde{v}^2 + \tilde{P}_1)\partial\tilde{v}/\partial\phi_2 + (V_1^* X_{12}/RT)[(2\theta_1 \theta_2^2/\tilde{v}\phi_1\phi_2) - (\theta_2^2/\tilde{v}^2)\partial\tilde{v}/\partial\phi_2] - (V_1^* Q_{12}/R)[2\theta_1 \theta_2^2/(\tilde{v}\phi_1\phi_2)] = 0 \tag{10}$$

where

$$\partial\tilde{v}/\partial\phi_2 = [\partial\tilde{P}/\partial\phi_2 - (1/\tilde{T})(\tilde{P} + 1/\tilde{v}^2)\partial\tilde{T}/\partial\phi_2] / \{ 2/\tilde{v}^3 - \tilde{T}(\tilde{v}^{1/3} - 2/3)/[\tilde{v}^{5/3}(\tilde{v}^{1/3} - 1)^2] \} \tag{11}$$

$$\partial\tilde{P}/\partial\phi_2 = [P_1^* - P_2^* + X_{12}\theta_2(\theta_1/\phi_2 - 1)]P/P^{*2} \tag{12}$$

$$\partial\tilde{T}/\partial\phi_2 = (P_2^*/T_2^* - P_1^*/T_1^*)T/P^* + [P_1^* - P_2^* + X_{12}\theta_2(\theta_1/\phi_2 - 1)]\tilde{T}/P^* \tag{13}$$

In order to use these equations the density d , the thermal expansion coefficient α and the thermal pressure coefficient γ or isothermal compressibility coefficient κ of the pure components are needed to evaluate the characteristic parameters P^* , T^* and v^* . We have

$$(\alpha T)^{-1} = 1/3(\tilde{v}^{1/3} - 1) - 1 + 2\tilde{P}\tilde{v}^2/(\tilde{P}\tilde{v}^2 + 1) \tag{14}$$

$$(\kappa P)^{-1} = [1/3(\tilde{v}^{1/3} - 1) - 1](1 + 1/\tilde{P}\tilde{v}^2) + 2 \tag{15}$$

$$\gamma T/P = 1 + 1/\tilde{P}\tilde{v}^2 \tag{16}$$

and the equation of state

$$\tilde{P}\tilde{v}/\tilde{T} = \tilde{v}^{1/3}/(\tilde{v}^{1/3} - 1) - 1/(\tilde{v}\tilde{T}) \tag{17}$$

At zero pressure the above relations become

$$\alpha T = 3(\tilde{v}^{1/3} - 1)/[1 - 3(\tilde{v}^{1/3} - 1)] \tag{18}$$

or

$$\tilde{v}^{1/3} - 1 = \alpha T/3(1 + \alpha T) \tag{19}$$

$$\kappa = 3(\tilde{v}^{1/3} - 1)\tilde{v}^2/[1 - 3(\tilde{v}^{1/3} - 1)]P^* = \alpha T\tilde{v}^2/P^* \tag{20}$$

$$\gamma = P^*/T\tilde{v}^2 \tag{21}$$

$$1/\tilde{T} = \tilde{v}^{4/3}/(\tilde{v}^{1/3} - 1) \tag{22}$$

\tilde{v} and P^* can be calculated from equations (14)–(16) or equations (18)–(21) using α and γ or κ . Then T^* can be calculated from the equation of state. The last step is to calculate v^* using d and \tilde{v} .

In calculating the phase boundary, the dependence of d , α , γ or κ on temperature and pressure should be considered.

$$v = 1/d \tag{23}$$

$$dv(T,P) = (\partial v/\partial T)_P dT + (\partial v/\partial P)_T dP \tag{24}$$

$$d\alpha(T,P) = (\partial\alpha/\partial T)_P dT + (\partial\alpha/\partial P)_T dP \tag{25}$$

$$d\gamma(T,P) = (\partial\gamma/\partial T)_P dT + (\partial\gamma/\partial P)_T dP \tag{26}$$

where

$$(\partial v/\partial T)_P = \alpha v \tag{27}$$

$$(\partial v/\partial P)_T = -\kappa v \tag{28}$$

$$(\partial\alpha/\partial T)_P = \tilde{v}^{1/3}\alpha^3 T/9(\tilde{v}^{1/3} - 1)^2 - \alpha/T - 4\tilde{P}\alpha^3 T\tilde{v}^2/(\tilde{P}\tilde{v}^2 + 1)^2 \tag{29}$$

$$= \alpha^2(7 + 4\alpha T)/3 \quad (P=0) \tag{30}$$

$$(\partial\alpha/\partial P)_T = -\tilde{v}^{1/3}\kappa\alpha^2 T/9(\tilde{v}^{1/3}-1)^2 - (1/P^* - 2\tilde{P}\kappa)2\tilde{v}\alpha^2 T/(\tilde{P}\tilde{v}^2 + 1)^2 \quad (31)$$

$$= \kappa(1 + \alpha T)(3 + 4\alpha T)/3T \quad (P=0) \quad (32)$$

$$(\partial\gamma/\partial T)_P = -\gamma(1 + 2\alpha T)/T + 2\alpha P/T \quad (33)$$

$$= -\gamma(1 + 2\alpha T)/T \quad (P=0) \quad (34)$$

$$(\partial\gamma/\partial P)_T = 1/T + 2\gamma\kappa - 2\kappa P/T \quad (35)$$

$$= 1/T + 2\gamma\kappa \quad (P=0) \quad (36)$$

S_1/S_2 can be obtained from crystallographic data⁹, by projecting a molecular model⁹, or using the group contribution technique of Bondi for computing van der Waals molecular volume and surface area¹⁰. χ_{12} can be evaluated from the heat of mixing

$$\Delta H_m = BN_1\phi_2 \quad (37)$$

$$B = \lim(\phi_2 \rightarrow 0)(\Delta H_m/N_1\phi_2)$$

$$= \lim(N_2 \rightarrow 0)(\Delta H_m/N_2)(V_1^*/V_2^*)$$

$$= (V_1^*/\tilde{v})\{P_2^*[\tilde{v}_1/\tilde{v}_2 - 1 - \alpha_1 T(1 - \tilde{T}_2/\tilde{T}_1)] + (1 + \alpha_1 T)(S_2/S_1)X_{12}\} \quad (38)$$

or the change in volume on mixing

$$\tilde{v}^0 = \phi_1\tilde{v}_1 + \phi_2\tilde{v}_2 \quad (39)$$

$$\tilde{v}^E = \tilde{v} - \tilde{v}^0 \quad (40)$$

$$\tilde{v}^E/\tilde{v}^0 = \Delta V_m/V^0 \quad (41)$$

EXPERIMENTAL

The systems studied were CPE/PMMA and COD/OMMA. Part of the experimental results have already been reported⁸. These include the phase diagram and the mechanical relaxation of polyblends, and the heat of mixing of oligomer pairs. In this paper we present data on the phase diagrams of some polyblends with higher molecular weight PMMA fractions, densities of the polyblends and the phase diagrams of oligomer mixtures.

Materials

PMMA F5 and F6 are fractions from a commercial product. They were dissolved in acetone (AR) and fractions were obtained by additions of acetone/water (1:1 volume ratio) at $25^\circ \pm 0.1^\circ\text{C}$. The fractions collected were redissolved in acetone, reprecipitated into water and dried in a vacuum oven at 1 mm Hg at 50°C for 1 week. The molecular weights were determined by g.p.c. in THF. All the molecular weights including those PMMA samples reported before⁸ have already been converted to PMMA using a universal calibration¹¹ and are given in Table 1. The details of other materials were described in the previous paper⁸. The molecular weights of COD were measured by vapour phase osmometry and compared

with the theoretical values calculated from the degrees of chlorination, as shown in Table 2.

The polyblends were prepared by casting films from MEK (AR) solutions in petri dishes. The rate of evaporation was controlled by partial covering. Because CPE 16, having the highest chlorine content, was used the mixtures were compatible at room temperature and the films were transparent. The films were dried in a vacuum oven at 1 mm Hg and 50°C for 1 week.

Phase boundaries of polyblends

The phase diagrams of the new systems CPE 16/PMMA F5 and CPE 16/PMMA F6 were measured by differential thermal analysis as before⁸. The method has an accuracy of $\pm 10^\circ\text{C}$.

In order to check the phase boundaries so measured CPE 16/PMMA 1.4 was studied by transmission electron microscopy using a JEM 100B machine. The blend had a weight fraction of 0.263 CPE and the temperature of phase separation was 140°C by d.t.a. Several strips of the blend were heated at 110° , 130° , 150° and 170°C for 15 min and then quenched before TEM observation. One strip of the blend without heat treatment was used as reference. The results are shown in Figure 1. The TEM observation verifies the phase boundary measured by d.t.a. It was observed that exposure under electron beam induced further phase separation in the sample which had already phase separated.

Density measurements

The density of the solid polyblend was determined by equal density titration. 3–4 fine pieces of polymer film were placed in a flask containing distilled water. The flask was kept at constant temperature in a bath maintained at $25^\circ \pm 0.1^\circ\text{C}$. Through a syringe a saturated sodium bromide solution was titrated in the flask until the film pieces floated in the solution, without sinking to the bottom or floating to the surface for several minutes. The density of the NaBr solution in the flask was presumed to have an equal density to the polymer. The density of the liquid was then measured using a pycnometer. The accuracy was estimated as $\pm 0.0005 \text{ g cm}^{-3}$ by repeat titrations.

Table 1 Molecular weights of PMMA samples

Sample	$M_w \times 10^{-4}$	$M_n \times 10^{-4}$
PMMA F5	26.4	15.4
F6	14.0	7.17
1.4	8.38	3.46
16	4.88	1.26
17	1.44	0.427

Table 2 Molecular weights of COD

Sample	Degree of chlorination, W_{Cl}	M from W_{Cl}	M_n by v.p.o.
COD 1	0.174	306	314
2	0.246	334	356
3	0.334	376	412
3A	0.349	385	421
4	0.432	438	467
5	0.529	523	546

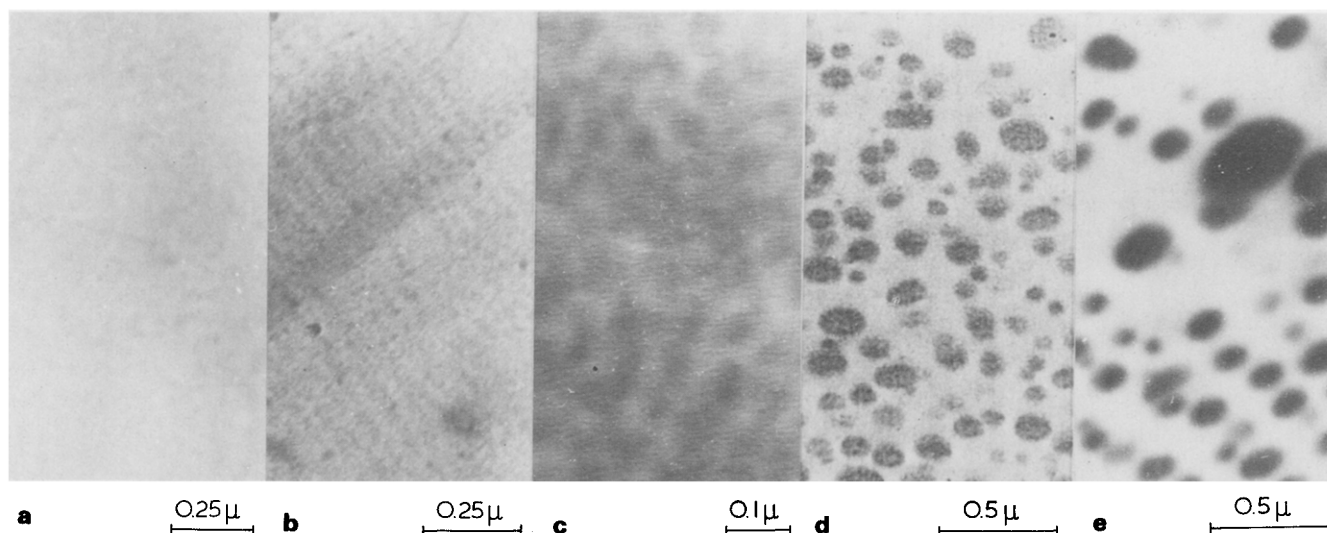


Figure 1 TEM observation of CPE 16/PMMA 1.4 samples treated at different temperatures. (a) Room temperature; (b) 110°C; (c) 130°C; (d) 150°C; (e) 170°C. The phase separation temperature is 140°C by d.t.a.

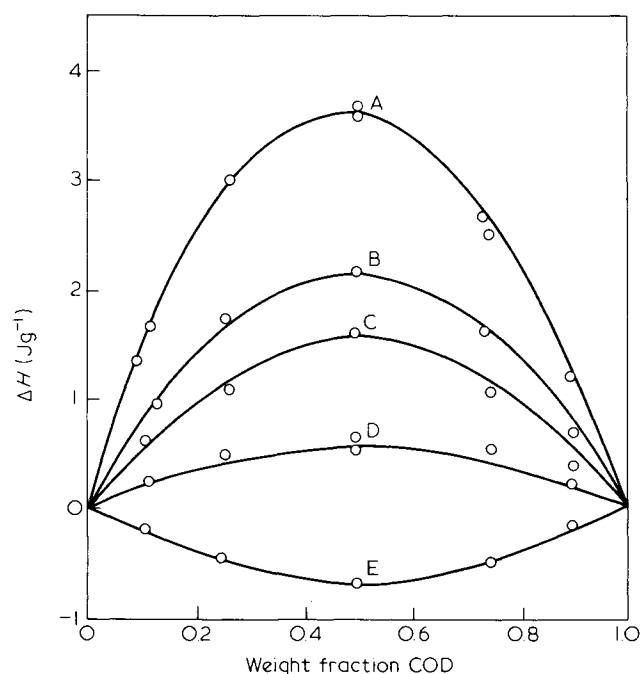


Figure 2 Heats of mixing for oligomeric PMMA (23) with chlorinated octadecanes plotted against weight fraction COD; A = COD 2 (24.6% Cl), B = COD 3 (33.7% Cl), C = COD 3A (34.9% Cl), D = COD 4 (43.2% Cl), E = COD 5 (52.9% Cl). The black lines are the theoretical curves by equation (2)

Phase boundaries of oligomer mixtures

Mixtures of oligomers were weighed in different proportions into glass tubes. The experiment was carried out in a silicone oil bath for mixtures of COD 1/OMMA 23 and COD 2/OMMA 23. The sample was heated over its cloud point by at least 10°C and mixed with a glass rod thoroughly. On cooling the mixture at 0.1°C/min, the cloud point was detected by the appearance of turbidity in the mixture. The measurement was repeated twice. Mixtures of COD 3/OMMA 23 were also studied and for these a methanol bath was cooled by a stream of nitrogen from a liquid nitrogen container. The cooling rate was controlled at 0.1°C/min by adjusting the nitrogen stream.

It was not possible to measure the phase boundaries of systems containing COD with high chlorine contents since the mixtures became viscous or solidified before any change was apparent. The accuracy of the phase boundary was estimated as 0.2°C for COD 1/OMMA 23 and COD 2/OMMA 23, and $\pm 2^\circ\text{C}$ for COD 3/OMMA 23 mixtures.

RESULTS AND DISCUSSION

Heats of mixing and phase boundaries of oligomers

Figures 2 and 3 show the experimental heats of mixing and the phase boundaries of COD/OMMA. The theoretical curves of ΔH_m also shown were calculated using equation (2). The experimental points are quoted from previous work⁸. With all the parameters fixed it was possible to adjust X_{12} to obtain a best ΔH_m curve to fit the experimental measurements. Table 3 shows the parameters used for the calculation.

The molecular weights were measured by vapour phase osmometry. The densities were measured using a pycnometer with an accuracy of $\pm 0.0002 \text{ g cm}^{-3}$ at 25°C and $\pm 0.0005 \text{ g cm}^{-3}$ at 70°C, respectively. α was estimated from the density measurements at two different temperatures with an accuracy of $\pm 0.15 \times 10^{-4} \text{ K}^{-1}$. γ was not available in the literature. It is known from the literature¹² that k of tetradecane at 20°C is $0.895 \times 10^{-4}/\text{atm}$, κ of dichloroethane at 20°C is $0.80 \times 10^{-4}/\text{atm}$. Hence κ of COD was set as $0.85 \times 10^{-4}/\text{atm}$. κ of OMMA was set at $1.00 \times 10^{-4}/\text{atm}$ after considering the κ value of PMMA¹³. γ was then calculated by equation (21). It was found that γ has little influence on the calculation. Changing γ of OMMA from 2 to 10 atm K^{-1} changes the value of ΔH_m calculated by about 2% and has virtually no effect on the phase boundary. The value of S_1/S_2 was estimated by Bondi's technique¹⁰, in which the correction for the case when the group is not attached to carbon is not considered. X_{12} was also calculated using equation (38). The value so obtained was within 5% of that from equation (2).

The spinodals were simulated using equation (10) with X_{12} evaluated from the heats of mixing. The value of X_{12}

for COD 1/OMMA 23 was an extrapolated value. It was found that if Q_{12} was set to zero the three systems discussed here would be miscible in the temperature range of interest. With Q_{12} as in Table 3 the spinodals simulated were in the right temperature range, but the experimental phase boundaries were asymmetric and the UCST was towards higher concentrations of COD.

Variation of X_{12} and Q_{12} with chlorine content

X_{12} and Q_{12} were plotted against the degree of chlorination of COD. The results are shown in Figure 4. X_{12} decreased linearly with increasing chlorine content in COD. Thus X_{12} can be separated into two terms as discussed by Paul¹⁴.

$$X_{12} = X_{12,dis} + W_{Cl}X_{12,sp} \quad (42)$$

The dispersion force $X_{12,dis}$ is around 340 atm, the specific interaction $X_{12,sp}$ is about -710 atm. With

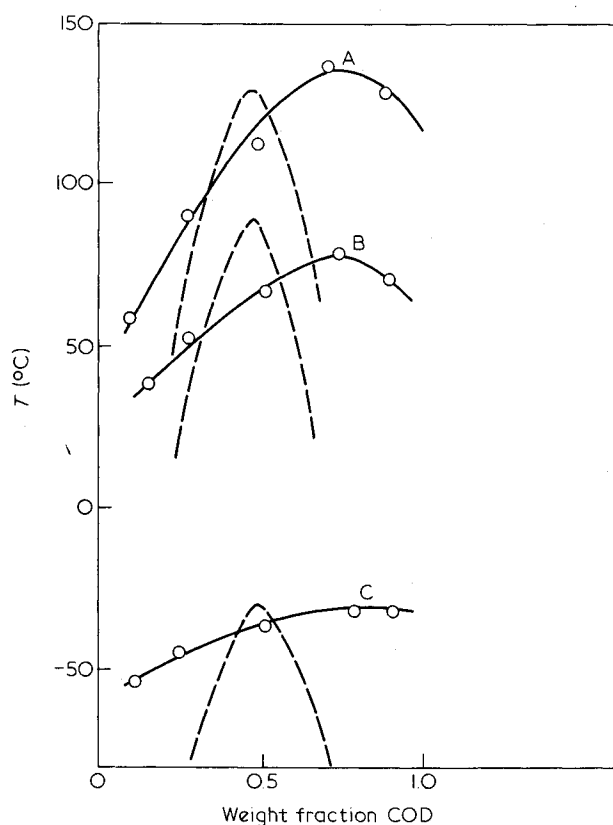


Figure 3 Phase diagram for oligomer mixtures; A = COD 1/OMMA 23, B = COD 2/OMMA 23, C = COD 3/OMMA 23. The broken lines are the simulated spinodals by equation (10)

increasing chlorine content the heat of mixing changes from endothermic to exothermic. Q_{12} is negative which suggests that the mixture has a more ordered structure compared to the pure substances. This could be caused by specific interactions between the two components in the mixture. Q_{12} also seems to have a dependence on the chlorine content in COD.

The shape of theoretical spinodals

It is impossible to move the theoretical UCST to the side of higher concentrations of COD by adjusting Q_{12} . Several other factors may influence our calculation.

(A) The molecular weights of the oligomers used for the calculation are number average values. In fact, the weight average value is a better measure for predicting the cloud point curve of polydisperse polymers¹⁵. We can assume that COD has a narrow molecular weight distribution because it was prepared by chlorination of octadecane. The molecular weights calculated according to their

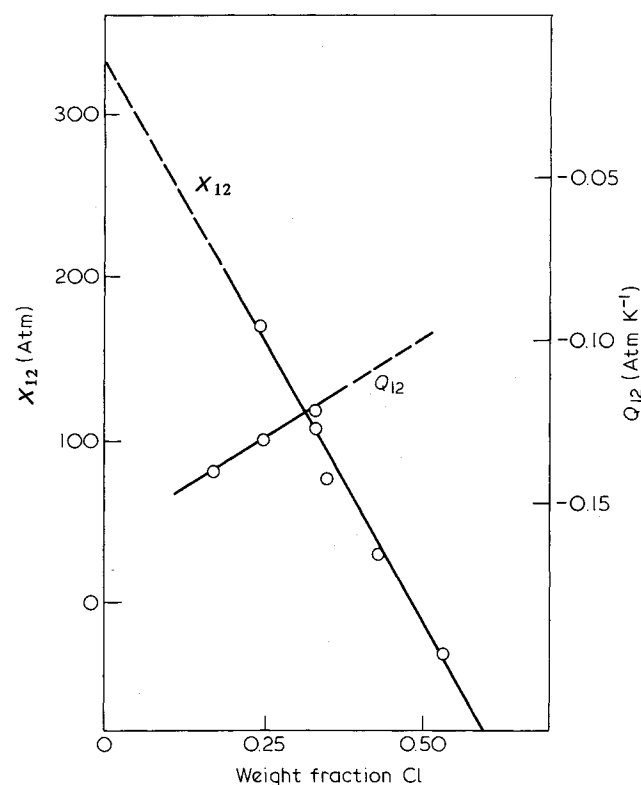


Figure 4 Values of the interaction energy parameter, X_{12} , and the interaction entropy parameter, Q_{12} , for mixtures of oligomeric PMMA with chlorinated octadecanes against the percentage chlorine in the chlorinated octadecane

Table 3 Parameters of oligomeric mixtures

	M_n	d (g cm ⁻³)		α ($\times 10^4$ K ⁻¹)	γ (atm. K ⁻¹)	S_1/S_2	X_{12} (atm.)	Q_{12} (atm. K ⁻¹)
		25°C	70°C					
1. COD 1	314	0.8976	0.8651	8.20	9.64	0.97	210	-0.14
2	356	0.9511	0.9180	7.87	9.26	0.96	170	-0.13
3	412	1.0531	1.0167	7.82	9.20	0.96	105	-0.12
3A	421	1.0807	1.0457	7.32	8.61	0.96	75	
4	467	1.1417	1.1054	7.18	8.45	0.95	30	
5	546	1.2579	1.2169	7.36	8.66	0.94	-35	
2. OMMA 23	434	1.1378	1.0889	9.76	9.76			

1 atm = 0.1013 J cm⁻³ = 0.02422 cal cm⁻³

chlorine contents are in agreement with the values measured by v.p.o. (see Table 2). This suggests that no disruption or extension of the basic chain structure occurs during chlorination. OMMA 23 was prepared by polymerization in the presence of a chain transfer agent. This produces a broad molecular weight distribution and hence probably a much higher M_w for this oligomer. If a larger M_w is used in the calculation the theoretical phase boundary will move to higher concentrations of COD because COD has a relatively low molecular weight.

(B) There can be irregular asymmetry in the phase boundary. This was referred to in the literature by Koningsveld *et al.*¹⁶ Some authors^{5,6} tried to explain the phenomenon using the equation of state theory. They concluded that if $X_{12} < 0$ and $S_1/S_2 < 1$, or $C_{12} > 0$ and $m_1/m_2 < 1$, an irregular asymmetric phase boundary will result. The number of external degrees of freedom per segment in the mixture, $3C$, is determined by

$$C = \phi_1 C_1 + \phi_2 C_2 - \phi_1 \phi_2 C_{12} \quad (43)$$

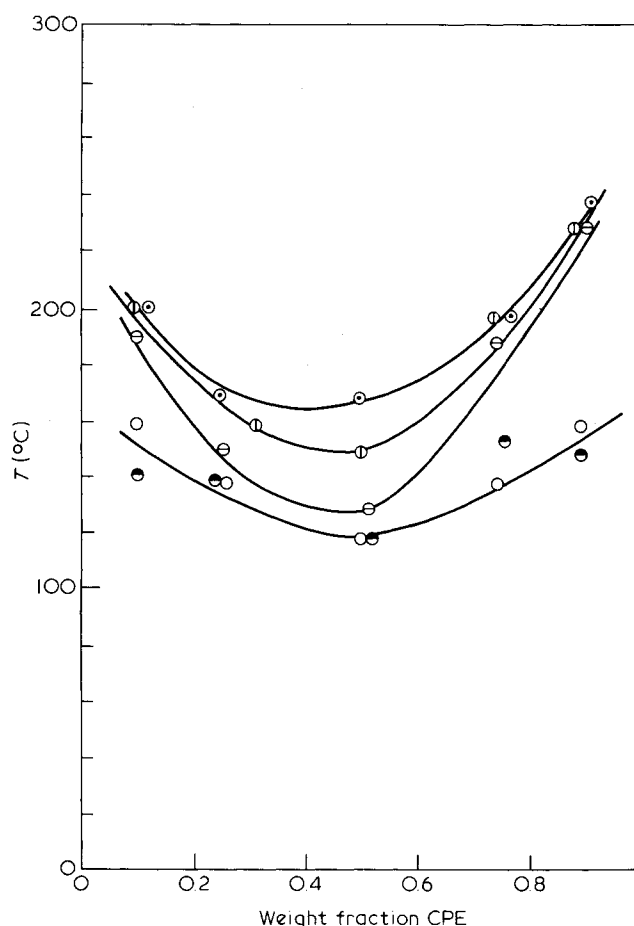


Figure 5 Experimental phase boundaries for mixtures of CPE 16/PMMA: \circ , PMMA 17; \square , PMMA 16; \triangle , PMMA 1.4; \circ , PMMA F6; \bullet , PMMA F5. The last two follow the same line within experimental error

Table 4 Parameters of CPE 16/PMMA blends

	M_w	d (g cm ⁻³) 30°C	α ($\times 10^4$ K ⁻¹)	γ (atm K ⁻¹)	S_1/S_2	X_{12} (atm.)	Q_{12} (atm. K ⁻¹)
1. CPE 16	19.8×10^4	1.400	5.45	10.00	0.94	-30	-0.06
2. PMMA	*	1.200	5.74	11.56			

* M_w of PMMA samples seen in Table 1

For COD/OMMA the condition $X_{12} < 0$ and $C_{12} > 0$ holds because of specific interactions. The condition $S_1/S_2 < 1$ and $m_1/m_2 < 1$ also holds from the geometry of the chain molecules.

Calculated and observed phase boundaries in high molecular weight blends

Figures 5 and 6 show the experimental phase boundaries and the simulated spinodals. In Figure 5 the phase boundaries for CPE 16/PMMA F5 and CPE 16/PMMA F6 are reported for the first time, those for other systems are quoted from a previous paper⁸. Table 4 shows the parameters used for the simulation.

Because the temperature range of interest is above 100°C, α values for $T > T_g$ were used for the calculation. γ of PMMA was also chosen to be the value when $T > T_g$. α and γ for PMMA come from the literature¹³. α for CPE 16 was evaluated from the densities observed at two temperatures and has an accuracy of $\pm 0.15 \times 10^{-4}$ K⁻¹. γ of CPE is not available in the literature; it was arbitrarily set as 10 atm K⁻¹. This parameter has little influence on the simulation. For example, when γ changes from 8 to 14 atm K⁻¹, (a range which covers most polymers), the phase boundary only changes 2°C. The value of S_1/S_2 of the oligomeric analogue was also used for high molecular systems. X_{12} was chosen as -30 atm, the value required to fit ΔH_m values of the oligomeric analogue with the same

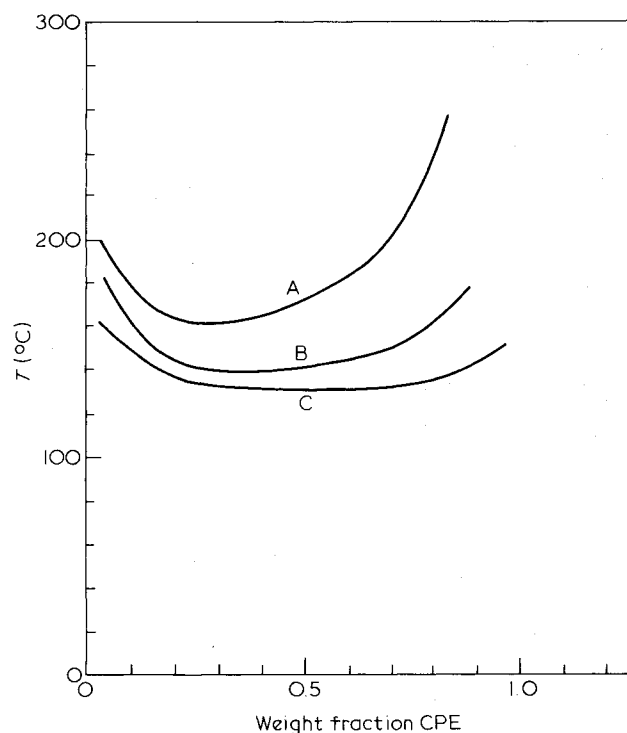


Figure 6 Simulated spinodals for mixtures of CPE 16/PMMA: A, PMMA 17; B, PMMA 16; C, PMMA F5

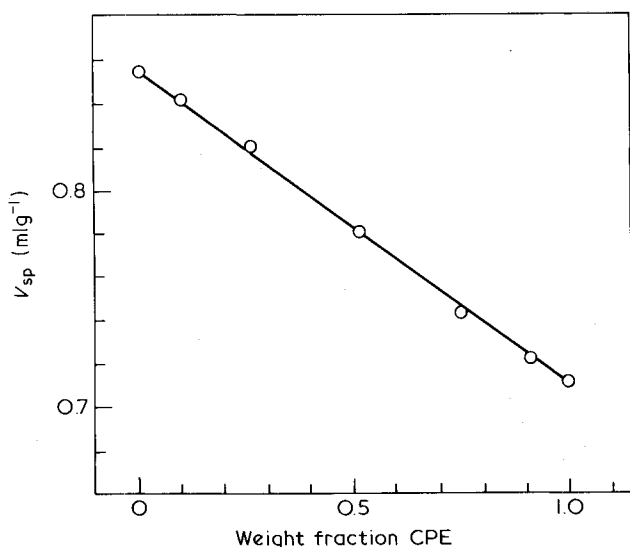


Figure 7 Specific volumes of CPE 16/PMMA 1.4 blends measured at $25^\circ \pm 0.1^\circ\text{C}$

chlorine content as CPE 16. Q_{12} was similarly chosen to be $-0.095 \text{ atm K}^{-1}$. It was found that the *LCST* so calculated for CPE 16/PMMA 1.4 was around 10°C , which was low compared to the experimental observation. Both X_{12} and Q_{12} have a large effect on the results. Since Q_{12} is an empirical parameter we adjust Q_{12} to fit the experimental phase boundary. When $Q_{12} = -0.06 \text{ atm K}^{-1}$ a satisfactory result is obtained. Considering that both X_{12} and Q_{12} may have molecular weight dependence, the adjustment of Q_{12} is acceptable. Another reason for accepting a higher Q_{12} value in high molecular weight polymer mixtures is that the values of Q_{12} from oligomeric analogues may be small because \overline{M}_n was used for simulation of the phase boundary. If \overline{M}_w values were used the Q_{12} values would be larger, and the value extrapolated to high chlorine content would also be higher.

The phase boundary simulated for high molecular weight polymer mixtures is flat-bottomed. The measurement of the *LCST* of the polymer mixture must therefore be done with great care, considering the inherent difficulty arising from the kinetic influence on phase separation of the system. In our experiment two polymers with high glass transition temperatures were studied, the phase separation thus proceeded slowly and gave only small phase sizes (about $\sim 10^3 \text{ \AA}$ by *TEM*). The method used in this paper for phase boundary determination is *d.t.a.*, which is not an accurate method for T_g measurements. For these two reasons the error in our phase boundary measurement is $\pm 10^\circ\text{C}$, which is not accurate enough to locate the position of an *LCST*.

The molecular weight dependence of the phase diagram

It was found that the calculated molecular weight dependence of the phase boundary conforms to the experimental observation. For example, when the molecular weight of PMMA increased from 1.44×10^4 to 26.4×10^4 , the *LCST* decreased by about 50°C , while the simulated spinodal decreased about 30°C . Compared to the large molecular weight dependence predicted by McMaster³, where $X_{12}=0$ and $Q_{12}=0$ were assumed, the improvement is apparent. From equation (10) for the spinodal we can see that in our system X_{12} and Q_{12}

counterbalance each other and suppress the combinatorial entropy term. Since they are less molecular weight dependent than the combinatorial entropy term, and we effectively ignored any possible molecular weight dependence in our discussion, the resultant phase boundary has less dependence on molecular weights.

Volume changes on mixing

The volume change of mixing was calculated using equation (41). The maximum theoretical $\Delta V_m/V^0$ is around 6×10^{-5} at a weight fraction of CPE of 0.5. This is in agreement with the density measurement. To an accuracy of 5×10^{-4} the specific volume was found to be additive depending only on the concentrations of the two compounds. Therefore $\Delta V_m/V^0$ must be smaller than 5×10^{-4} , showing that a very weak interaction exists in the mixture. The experimental results for the specific volumes of polyblends are shown in Figure 7.

CONCLUSIONS

Investigation of the effect of chlorine content on the heats of mixing of oligomer mixtures of COD/OMMA shows that there are two kinds of interactions in the system: dispersion forces and specific interactions. Both the interaction energy parameter X_{12} and the interaction entropy parameter, Q_{12} , are dependent on the chlorine content in COD. The thermodynamic parameters X_{12} and Q_{12} obtained from oligomer models can be used to generate the phase boundary of high polymer mixture. Because the interaction contributions, which are less molecular weight dependent, suppress the contribution of the combinatorial entropy, the phase boundaries so generated are less molecular weight dependent than the case when $X_{12}=0$ and $Q_{12}=0$, and in better agreement with the experimental observation. The negative value of Q_{12} indicates that some ordered structure may exist in both high and low molecular weight mixtures compared to their pure components. The results show that simulation of a polymer mixture by oligomeric analogues is a valuable method in the thermodynamic study of miscibility.

ACKNOWLEDGEMENT

We would like to thank Sir Geoffrey Allen for his valuable suggestions. One of us (CZ) would like to express his thanks to the SERC and Academia Sinica for research grants.

REFERENCES

- 1 Abe, A. and Flory, P. J. *J. Am. Chem. Soc.* 1966, **88**, 2887
- 2 Flory, P. J., Eichinger, B. E. and Orwoll, R. A. *Macromolecules* 1968, **1**, 287
- 3 McMaster, L. P. *Macromolecules* 1973, **6**, 760
- 4 Patterson, D. and Robard, A. *Macromolecules* 1978, **11**, 690
- 5 Olabisi, O. *Macromolecules* 1975, **8**, 316
- 6 tenBrinke, G., Eshuis, A., Roerdink, E. and Challa, G. *Macromolecules* 1981, **14**, 867
- 7 Allen, G., Gee, G. and Nicholson, J. P. *Polymer* 1961, **2**, 8
- 8 Walsh, D. J., Higgins, J. S. and Chai, Z. *Polymer* 1982, **23**, 336
- 9 Eichinger, B. E. and Flory, P. J. *Trans. Faraday Soc.* 1968, **64**, 2035, 2053
- 10 Bondi, A. *J. Phys. Chem.* 1964, **68**, 441
- 11 Evans, J. M. *Polym. Eng. Sci.* 1973, **13**, 401
- 12 Allen, G., Gee, G. and Wilson, G. J. *Polymer* 1969, **1**, 456
- 13 Brandrup, J. and Immergut, E. H. 'Polymer Handbook', Wiley, 1975

- 14 Paul, D. R. 'Polymer Blends', (Eds. D. R. Paul and S. Newman), Academic Press, 1978, Vol. 1, Ch. 1
 15 Nishi, T. and Kwei, T. K. *Polymer* 1975, **16**, 285
 16 Koningsveld, R., Kleintjens, L. A. and Schoffeleers, H. M. *Pure. Appl. Chem.* 1974, **39**, 1

APPENDIX

Symbols used in equations (1-42)

B	an assumed constant as defined in equation (37)	\bar{r}	average number of segments in mixture defined as $\bar{r}N = \sum r_i N_i$
d	density	S_i	number of contact sites per segment in species i
ΔG_m	free energy of mixing	ΔS_m	entropy of mixing
ΔH_m	heat of mixing	T	temperature
N	total number of molecules in mixture	T_i^*	characteristic temperature of species i
N_i	number of molecules in species i	\tilde{T}_i	reduced temperature of species i , $\tilde{T}_i = T/T_i^*$
n_i	molar number of species i	T^*	characteristic temperature of mixture
P	pressure	\tilde{T}	reduced temperature of mixture
P_i^*	characteristic pressure of species i	v	specific volume
\tilde{P}_i	reduced pressure of species i , $\tilde{P}_i = P/P_i^*$	v_i^*	characteristic volume of species i
P^*	characteristic pressure of mixture	\tilde{v}_i	reduced volume of species i , $\tilde{v}_i = v_i/v_i^*$
\tilde{P}	reduced pressure of mixture	v^*	characteristic volume of mixture
Q_{12}	interaction entropy parameter	\tilde{v}	reduced volume of mixture
R	gas constant	\tilde{v}^0	additive reduced volume as defined in equation (39)
r_i	number of segments in chain molecule i	\tilde{v}^E	excess reduced volume
		V^0	total volume of mixture
		ΔV_m	volume change of mixing
		X_{12}	interaction energy parameter
		α	thermal expansion coefficient
		γ	thermal pressure coefficient
		κ	isothermal compressibility coefficient
		$\Delta\mu_i$	chemical potential of species i
		ϕ_i	segment fraction of species i
		θ_i	site fraction of species i